Kure Tekko magnet wankel motor reexamined

J.L. Duarte
Dept. Electrical Engineering (Ret.)
Eindhoven University of Technology
The Netherlands

***Abstract*—The exceptional performance observed in past demonstrations with the Kure Tekko "magnetic Wankel" — where efficiencies exceeding 100% were reported — might be attributed to mechanical vibrations in the motor shaft rather than to the influence of a spiral-shaped magnetic field gradient.**

I. Introduction

A peculiar electromagnet/permanent magnet motor for electric cars, nicknamed "magnetic Wankel", was introduced in 1979 in Japan, based on a magnetic propulsion concept [1]. It was professionally designed and manufactured by Kure Tekkosho K.K., a manufacturer of automotive components.

Although the account in [1] states that "no performance details have been revealed," both power (33 kW) and weight (75 kg) are given. This suggests that the motor had a superior power-to-weight ratio compared to conventional engines available at the time (about 200 kg for similar power). At first sight, it is remarkable that the most crucial performance indicator—efficiency—is not mentioned. Nevertheless, if an efficiency exceeding 100% had been achieved, omitting such a provocative result would be more comprehensible.

The Kure Tekko motor was designed and built to outperform conventional motors significantly. This has sparked some interest and investigation [2]. Yet, in the absence of an understandable description allowing independent reproduction, the concept has remained at a standstill.

Building on the vibrational model proposed in [4, Part III], we show in Section II that the Kure Tekko motor exhibits characteristics of a magnetic mill and shares noteworthy similarities with [5]. In Section III we give an overview of the propulsion forces, with implications to the process of energy unfolding. Then, in Section IV we draw conclusions based on the fundamental principles underlying both motors.

II. Wankel motor concept

With regards to [1] and a series of patents filed by the manufacturer [3], the "magnetic Wankel" operates on a spiral magnetic field gradient, as outlined in Fig. 1.

In this design concept, the rotor, equipped with magnet segments, rotates within a stator that features a spiral-shaped arrangement of permanent magnets. As the rotor moves along the spiral, mutual magnetic repulsion accelerates it.

At the end of the spiral, a gap interrupts the motion, requiring the rotor to cross it before continuing its cycle. To facilitate this transition, an electromagnet (a solenoid) is activated to propel the rotor across the gap, consuming electrical energy in the process.

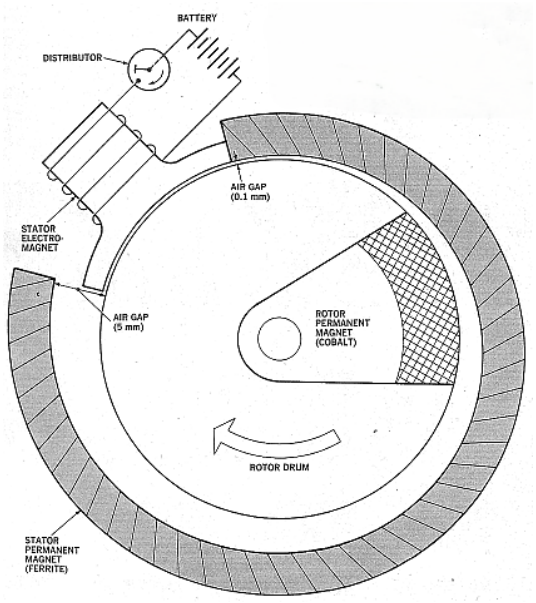

Fig. 1: Electromagnetic propulsion in a Kure Tekko "wankel" motor as sketched in [1].

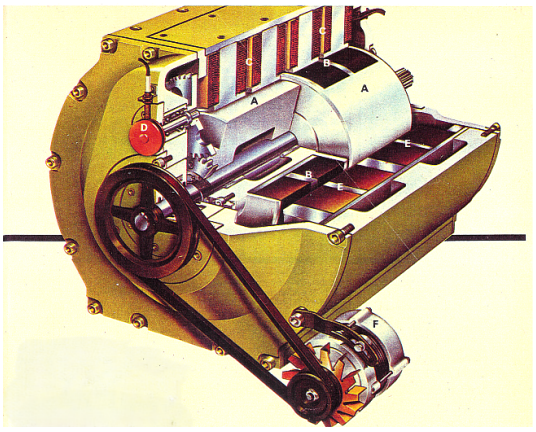

Fig. 2: Impression from [1], showing staggered rotor drums (A) with magnets (B), electromagnet coils (C), gear-driven distributor (D), stator spiral assembly (E), auxiliary drive (F).

In the sequel, excerpts with details of the motor concept are commented (see Fig. 2):

- *"The experimental 45-hp rotary engine uses two separated rotor drums, each with three cobalt magnets, separated 60 degrees apart . . . Each cobalt magnet spans*

a narrow 60-degree sector of the rotor's circumference ... The cobalt magnet segments are so angled on the common shaft that there's equal radial spacing around the circle" ([1], p. 81).

In other words, three cobalt magnet segments are radial spaced by 120 degrees at each rotor drum. Moreover, two drums are angular staggered by 60 degrees. Consequently, the arrangement of the rotor drums creates a 3D helical magnetic field gradient.

- *"The drums spin within a stator ring composed mainly of a permanent ferrite magnet. But the stator has a 60-degree gap spanned by electromagnets"* ([1], p. 80).

  It is suggested in Fig. 1 that the stator ring is not assembled with just one single monolithic structure to get a tapered shape, but by means of slanted magnet segments, as expected from a practical point of view [3]. Therefore, because of some angular spacing between magnet segments, the resulting magnetic flux density in the radial direction comports a ripple on top of the main spiral component ([3], p. 36). Accordingly, this ripple is synchronously superposed on the helical magnetic field gradient as a multiple of the angular frequency.
- *"Each rotor drum spins past its own stator electromagnet that is "fired" by the gear-driven distributor. The multi-point distributor gives six power impulses per revolution to kick each of the three cobalt magnet segments along. They are propelled the rest of the way by the magnetic forces generated between them and the eccentrically shaped stator rings that cause an ever-widening air gap to face the magnets"* ([1], p. 81).

  Which is to say, a distributor sensing the rotor angular position regulates the electric-current flow to the corresponding electromagnet coil, briefly energizing it precisely as a cobalt magnet segment passes by. As a side effect, at each 60-degree of the angular frequency, an electric-current impulse creates extra magnetic flux ripple on the helical field gradient, also in synchrony with the angular rotation.

  The short electric-current impulses do put energy into the system, but they were not energetic enough to explain an achieved output power in the kilowatt range. Since working prototypes had been successfully demonstrated, an efficiency exceeding 100% was, therefore, to be expected.

Altogether, the Kure Tekko motor shares a common ground with other magnetic mills [5] [6]:

- The angular staggering of rotor magnets in the circumferential direction forms the basis of a helical magnetic field gradient, being one of the necessary conditions to get resonances in spacetime [4, Part II].
- The (even small) spacing between stator magnets creates a B-field ripple, superimposed on the helical field gradient, which is in synchrony with the angular rotation[1]. Moreover, the six electric-current impulses, also aligned with the rotation, generate additional B-field ripple. As a consequence, spacetime resonances are evoked, leading to circularly polarized magnetic waves [4, Part II].
- In the environment where spacetime resonances occur, angular mechanical vibrations appear in the rotor shaft, which are correlated to the rate-of-change of generated impulsive magnetic forces, allowing scavenging of energy from the quantum vacuum field [4, Part III].

[1]Alike situation as in [5, Fig.2] and [6].

III. Improved propulsion

A first-order description of forces in the Kure Tekko motor follows, in line with the analysis in [5][2], showing the conditions for energy unfolding.

A. Magnetic force components

For the sake of simplification, let's consider in Fig. 1 that both, the elementary magnetic dipoles in the rotor, $\vec{\mu}_C$, and the external B-field actuating on them, $\vec{B}_{\text{ext}}$, are radial, as in [4, Part III, Eq.(8)]:

$$\vec{\mu}_C = \mu_C \, \vec{a}_r \,, \tag{1}$$

$$\vec{B}_{\text{ext}} = (B_S + B'_S \cos(\eta\phi) + B''_S(\phi)) \, \vec{a}_r \,, \tag{2}$$

for which

$$\vec{a}_r = \cos\phi \, \vec{a}_x + \sin\phi \, \vec{a}_y \,,$$

$$\vec{a}_\phi = -\sin\phi \, \vec{a}_x + \cos\phi \, \vec{a}_y \,,$$

are referenced to Cartesian orthonormal vectors $(\vec{a}_x, \vec{a}_y)$, and ϕ is the rotation angle with respect to $\vec{a}_x$.

In (2), the term B_S describes the magnitude of a circularly polarized wave with Beltrami structure, which is evoked from spacetime resonances, owing to matched magnetic field disturbances.

The modulation term $B'_S \cos(\eta\phi)$, added to the carrier magnitude B_S, represents an approximation of magnetic field disturbances that occurs in synchrony with the rotor's angular velocity. As said, in the Kure Tekko motor, these disturbances have two components from different origins – the electromagnet electric-current impulses and the angular spacing between stator magnet segments. To simplify the analysis, each ripple component can be separately taken into consideration, because, in the end, the resulting forces, owing to particular values[3] of η in $B'_S \cos(\eta\phi)$, can be linearly added.

The extra term $B''_S(\phi)$ in (2) is a result of the spiral magnet arrangement of the stator. It describes a linearly growing and decaying gradient in anti-radial direction (as opposed to $\vec{\mu}_C$, therefore the negative sign) given by

$$B''_S(\phi) = \begin{cases} -\left(B^{\min} + \dfrac{B^{\max} - B^{\min}}{\xi\pi}\phi\right) & \text{if } 0 < \phi < \xi\pi \\ -\left(B^{\max} - \dfrac{B^{\max} - B^{\min}}{2\pi - \xi\pi}(\phi - \xi\pi)\right) & \text{if } \xi\pi < \phi < 2\pi \end{cases} \tag{3}$$

where ξ delimits the angular region below the electromagnet ($\xi = 1/3$ in Fig. 1), where an electric-current impulse boosts the gap B-field from $B^{\min}$ to $B^{\max}$.

[2]The nomenclature in [4, Part III] and [5] are equally applicable here.

[3]For instance, $\eta = 6$ corresponds to six electric-current impulses, or η is equal to the number of magnet segments in the stator spiral.

Regarding separately the effect of $B''_S(\phi)$ in (2), the magnetic force acting on $\vec{\mu}_C$ is found with

$$\vec{\nabla}\left([\mu_C\,\vec{a}_r]\cdot[B''_S(\phi)\,\vec{a}_r]\,\right)=\vec{\nabla}(\mu_C B''_S(\phi)\,). \tag{4}$$

For circular motion of $\vec{\mu_C}$, respecting Cartesian coordinates $(x_C = r_C\cos\phi\,, y_C = r_C\sin\phi)$, the angular force on the magnetic momentum follows from (4), after some manipulations, as

$$\vec{F}''_\phi=\frac{2\mu_C}{r_C}\frac{\partial B''_S(\phi)}{\partial\phi}\,\vec{a}_\phi=F''_\phi\,\vec{a}_\phi \tag{5}$$

with, in view of (3),

$$F''_\phi=\begin{cases}-\dfrac{1}{\xi\pi}F''_0 & \text{for } 0<\phi<\xi\pi\\[2mm] \dfrac{1}{2\pi-\xi\pi}F''_0 & \text{for } \xi\pi<\phi<2\pi\end{cases} \tag{6}$$

and

$$F''_0=\frac{2\mu_C\left(B^{\max}-B^{\min}\right)}{r_C}. \tag{7}$$

Consequently, $\vec{F}''_\phi$ is piece-wise constant, and the net mechanical work done in circumferential direction per rotation cycle is found to be

$$\int_0^{\xi\pi}F''_\phi r_C\,d\phi+\int_{\xi\pi}^{2\pi}F''_\phi r_C\,d\phi=0\,, \tag{8}$$

as expected. However, if angular disturbances are considered, then $\vec{F}''_\phi$ does affect the transfer of energy from the quantum vacuum, as follows.

B. Energy increments

According to [4, Part III, Eq.(22)], angular disturbance increments on the motor shaft are assumed correlated to impulsive radial forces as

$$d\phi'_S=\lambda\frac{\partial F_r}{\partial\phi}d\phi, \tag{9}$$

where F_r is given by [4, Part III, Eq.(19)]

$$F_r(\phi)=\left(\frac{2\eta\mu_C B'_S}{r_C}\right)\frac{\sin(\eta\phi)\cos(2\phi)}{\sin(2\phi)}. \tag{10}$$

The work done by the circular force $\vec{F}''_\phi$ on $\vec{\mu}_C$, along with vibrational increments[4], adds an infinitesimal energy drop to the motor shaft as

$$dQ''_S=F''_\phi\,r_C\,d\phi'_S. \tag{11}$$

Hence, the net scavenged energy per revolution follows from (9) and (11) as

$$Q''_S=\,r_C\lambda\left(\int_0^{\xi\pi}F''_\phi\frac{\partial F_r}{\partial\phi}d\phi+\int_{\xi\pi}^{2\pi}F''_\phi\frac{\partial F_r}{\partial\phi}d\phi\right). \tag{12}$$

Since $F_r(2\pi)=F_r(0)$, substitution of (6) into (12) leads to

$$Q''_S=\,r_C\lambda F''_0\left(\frac{1}{\xi\pi}+\frac{1}{2\pi-\xi\pi}\right)\Big(F_r(0)-F_r(\xi\pi)\Big). \tag{13}$$

[4]It should be noted that the value of B'_S in (10), which is implicit in (9), is related to the magnetic ripple disturbance, and not to the stator's spiral shape.

Subsequently, in view of (7) and (10),

$$Q''_S=Q''_0\left(\frac{\eta}{2}-\frac{\sin(\eta\xi\pi)\cos(2\xi\pi)}{\sin(2\xi\pi)}\right) \tag{14}$$

with

$$Q''_0=8\frac{\eta\,\lambda\mu_C^2B'_S\left(B^{\max}-B^{\min}\right)}{r_C\,(2-\xi)\xi\pi} \tag{15}$$

In case of $\eta=6$ and $\xi=1/3$, follows $Q''_S=3\,Q''_0$.

For the sake of comparison, regarding separately the effect of $B'_S\cos(\eta\phi)$ in (2), the net scavenged energy per revolution is found from [4, Part III, Eq.(28)] to become

$$Q'_S=Q'_0\int_0^{2\pi}\frac{\sin(\eta\phi)}{\sin(2\phi)}\left[2\frac{\sin(\eta\phi)}{\sin(2\phi)}-\eta\cos(\eta\phi)\cos(2\phi)\right]d\phi \tag{16}$$

with

$$Q'_0=8\frac{\lambda(\eta\mu_C B'_S)^2}{r_C}\,. \tag{17}$$

For $\eta=6$, follows $Q'_S=18.84\,Q'_0$.

C. Auxiliary drive

In Fig. 2, an extra motor is included (*F*), mentioned in [1] as a "small electric motor" that "crank-starts" the system, being mechanically connected to the Kure Tekko motor shaft via a pulley/belt drive. By visual appearance, it matches a typical continuously-running automotive alternator, rather than a starter motor only. Furthermore, there is no mention of a method disconnecting this auxiliary drive.

When compared to the total generated output power in the kilowatt range, it is evident that this alternator — when operating as a motor — delivers only a small amount of mechanical energy to the shaft, sufficient merely to offset minor losses and maintain the magnet motor in stable continuous operation.

An auxiliary belt–pulley drive is also found in other magnetic mill configurations, particularly at higher output powers [6]. As suggested in Fig. 2, adjusting the belt span is expected to help stabilize power generation while accommodating mechanical angular shaft vibrations. In the recorded presentation of [6], the inventor also emphasizes this point with the advice: "not too tight, not too loose!"

IV. Conclusion

The superior performance observed in the past with Kure Tekko motors cannot be explained solely by the propulsion given by a spiral magnetic field gradient. In accord with [4], owing to a magnetic flux ripple disturbing the rotor's helical magnetic field gradient, a process occurs in which energy is extracted from the quantum vacuum field through mechanical vibrations.

The sources of magnetic flux ripple in a Kure Tekko motor are the aligned electromagnet current impulses and the spacing in-between magnet segments in the stator. As such, the separation of magnet segments is not a drawback but rather an essential, not yet explored, design parameter for assembling magnetic mills.

ACKNOWLEDGEMENTS

The personal communications with Horst Eckardt were greatly appreciated.

REFERENCES

[1] D. Scott, *Magnetic "Wankel" for electric cars*, Popular Science magazine, June, 1979, pp. 80-81

[2] T. Valone, *Permanent Magnet Spiral Motor for Magnetic Gradient Energy Utilization: Axial Magnetic Field*, Space, Propulsion & Energy Sciences Int. Forum (SPESIF), Appl. Physics Lab – John Hopkins Univ., Feb. 23, 2010, 14 pp. https://www.researchgate.net/publication/228774077

[3] T. Loder, *Experiments with Spiral Magnetic Motors*, Int. Conf. on Future Energy II, March 19, 2012, 46 pp. https://www.omforum.cz/soubory/sfo16/loderspiralmotor-omf5042.pdf

[4] J.L. Duarte, *Essay on magnetic-wind mills - Parts I-II-III*, TU Eindhoven Research Report, Dec 10, 2024 https://research.tue.nl/en/publications/essay-on-magnetic-wind-mills-parts-i-ii-iii

[5] J.L. Duarte, *Howard Johnson magnet motor reexamined*, AIAS - Publications - Electromagnetic ECE Theory, Dec. 2024 https://aias.institute/3-Scientific-Work/Publications.html

[6] *Dicas do Leao - recorded demo video's*, 2023 https://github.com/JLDuarte55/magnetogenesis

Eindhoven, October 8, 2025